VIETNAM NATIONAL UNIVERSITY HO CHI MINH CITY
HO CHI MINH CITY UNIVERSITY OF TECHNOLOGY

Nguyen Thi Xuan Huynh

HYDROGEN STORAGE IN METAL-ORGANIC FRAMEWORK MIL-88S: A COMPUTATIONAL STUDY

Major: ENGINEERING PHYSICS
Major code: 62520401

PhD Dissertation - Summary

Ho Chi Minh City – 2019

The dissertation was completed in Ho Chi Minh City University of Technology, Vietnam National University – Ho Chi Minh city.

Scientific Supervisor 1: Dr. Do Ngoc Son

Scientific Supervisor 2: Dr. Pham Ho My Phuong

Independent Reviewer 1: Assoc. Prof. Dr. Pham Tran Nguyen Nguyen

Independent Reviewer 2: Assoc. Prof. Dr. Nguyen Thanh Tien

Reviewer 1: Assoc. Prof. Dr. Phan Bach Thang

Reviewer 2: Assoc. Prof. Dr. Huynh Quang Linh

Reviewer 3: Dr. Phan Hong Khiem

The dissertation will be defended in front of the board of examiners at .....
.....
.....
on .....

This dissertation can be found at following libraries:
- The Library of the Ho Chi Minh City University of Technology, VNU-HCM
- Central Library – VNU HCM
- General Science Library – Ho Chi Minh City

LIST OF PUBLICATIONS

I. Journal articles

[1] N. T. X. Huynh, C. Viorel**,** and D.N. Son, "Hydrogen storage in MIL-88 series," *Journal of Materials Science*, vol. 54, pp. 3994-4010, 2019 (Q1, IF = 3.442).

[2] N. T. X. Huynh, O M. Na, C. Viorel**,** and D.N. Son, "A computational approach towards understanding hydrogen gas adsorption in Co-MIL-88A," *RSC Advances*, vol. 17, pp. 39583-39593, 2017 (Q1, IF = 3.049)c.

[3] T. T. T. Huong, P. N. Thanh, N. T. X. Huynh, and D. N. Son, "Metal-Organic Frameworks: State-of-the-art Material for Gas Capture and Storage," *VNU Journal of Science: Mathematics – Physics*, vol. 32, pp. 67-84, 2016.

II. Conference reports

[1] D. N. Son, N. T. X. Huynh, P. X. Huong, P. N. Thanh, P. N. K. Cat, and M. Phuong Pham-Ho, CO_2 capture in metal organic framework MIL-88s by computational methods, International Symposium on Applied Science (ISAS), Ho Chi Minh City University of Technology (HCMUT), 2019 (accepted).

[2] N. T. X. Huynh, P. X. Huong, and D. N. Son, Hydrogen storage and carbon dioxide capture in metal organic framework M-MIL-88A (M = Sc, Ti, V, Fe), First Rencontres du Vietnam on Soft Matter Science, ICISE, Quy Nhon city, Vietnam, 2019.

[3] N. T. X. Huynh, O. K. Le, and D. N. Son, "Hydrogen storage in metal organic framework MIL-88D," *The 43rd National Conference on Theoretical Physics (NCTP-43)*, Quy Nhon city, Vietnam, 2018.

[4] N. T. X. Huynh, O M. Na, and D. N. Son, "Computational study of hydrogen adsorption in MIL-88 series," *The 42nd National Conference on Theoretical Physics (NCTP-42)*, Can Tho city, Vietnam, 2017.

[5] D. N. Son, N. T. X. Huynh, and O M. Na, "Exploring Hydrogen Gas Adsorption in Co-MIL-88A by Computational Methods," *The 42nd National Conference on Theoretical Physics (NCTP-42)*, Can Tho city, Vietnam**,** 2017.

[6] N. T. Y. Ngoc, N. T. X. Huynh, and D. N. Son, "Investigation of hydrogen adsorption in M(bdc)$(ted)_{0.5}$ by computer simulation methods," *The 42nd National Conference on Theoretical Physics (NCTP-42)*, Can Tho city, Vietnam, 2017.

[7] P. X. Huong, N. T. X. Huynh, and D. N. Son, "Adsorption of CO_2 in metal-organic framework of MIL-88A by computational methods," *The*

42nd National Conference on Theoretical Physics (NCTP-42), Can Tho city, Vietnam, 2017.

[8] N. T. X. Huynh, O M. Na, and D. N. Son, "Influence of trivalent transition metals in MIL-88A on hydrogen sorption," *Scientific and technological conference for young researchers - Ho Chi Minh City University of Technology*, HCM city, Viet Nam, 2017.

[9] N. T. X. Huynh, O M. Na, and D. N. Son, "Effects of metal substitution in MIL-88A on hydrogen adsorption: Computational study," *The Third International Conference on Computational Science and Engineering (ICCSE-3)*, Ho Chi Minh city, Vietnam, 2016.

[10] T. T. T. Huong, P. N. Thanh, N. T. X. Huynh, D. N. Son, "Metal – organic frameworks: Potential applications and prospective future research," *The 14th Conference on Science and Technology: International Symposium on Engineering Physics and Mechanics, Ho Chi Minh City University of Technology*, HCM city, Vietnam, 2015.

III. Research projects

[1] Hydrogen and carbon dioxide sorption in metal-organic frameworks of MIL-88 series: Computational study, Code number: **103. 01-2017.04**, Nafosted Funding, 2017 – 2019 (Research role: *PhD student*).

[2] Theoretical study of the propagation and the Anderson localization of waves in complex media, Code number: **103. 01-2014.10**, Nafosted Funding, 03/2015 – 03/2017 (Research role: *Technician*).

[3] Hydrogen gas adsorption in MIL-88A(Co): A density functional theory study, Code number: **TNCS-2015-KHUD-33**, 2015-2017 (*Co-principal investigator*).

[4] Study the adsorption capacity of hydrogen gas in Metal-organic frameworks by simulation method, Code number: **T2015.460.05**, Quy Nhon University, 2015-2016 (*Principal investigator*).

IV. Others

[1] N. T. X. Huynh, C. Viorel**,** and D.N. Son, *"Effect of metal substitution in MIL-88A on hydrogen adsorption: Multi-scale theoretical investigation"* in preparation.

[2] N. T. X. Huynh, C. Viorel**,** and D.N. Son, *"Hydrogen storage and carbon dioxide capture in M-MIL-88D metal-organic framework family"* in preparation.

ABSTRACT

Fossil fuel-based energy consumption causes serious environmental impacts such as air pollution, greenhouse effect, and so on. Therefore, searching clean and renewable energy sources is urgent to meet the demand for sustainable development of the global society and economy. Hydrogen gas (H_2) is a reproducible, clean, and pollution-free energy carrier for both transportation and stationary applications. Hydrogen gas has a much higher energy density than other fuels; and thus, it becomes one of the most promising candidates to replace petroleum. Therefore, in recent years, the interest in the research and development of hydrogen energy has grown constantly. A safe, efficient, and commercial solution for hydrogen storage is based on adsorption in porous materials, which have the exceptionally large surface area and ultrahigh porosity such as metal-organic framework (MOF) materials. In order to be selected as porous materials for gas storage, MOFs must be stable to avoid collapsed under humid conditions. MIL-88 series (abbreviated as MIL-88s including MIL-88A, MIL-88B, MIL-88C and MIL-88D) is highly stable and flexible sorbents. For these reasons, MIL-88s becomes a suitable candidate for the storage of hydrogen gas based on the physisorption. Moreover, coordinatively unsaturated metal centers in MIL-88s are able to enhance gas uptakes significantly at ambient temperatures and low pressures. These materials have been investigated and highly evaluated for various applications such as gas storage/capture and separation of binary gas mixtures in recent years; however, they have not yet been evaluated for hydrogen storage. These outstanding features have attracted my attention to consider the hydrogen storage capacity in MIL-88 series.

In this dissertation, the van der Waals dispersion-corrected density functional theory (vdW-DF) calculations were used to examine the stable adsorption sites of the hydrogen molecule in MIL-88s and clarify the interaction between H_2 and MIL-88s via electronic structure properties. This observation showed an implicit role of electronic structures on the H_2 adsorption capacity at the considered temperature and pressure conditions. Besides, it was found that the H_2@MIL-88s interaction is dominated by the bonding state (σ) of the hydrogen molecule and the *p* orbitals of the O and C atoms in MIL-88s. For MIL-88A and B, the *d* orbitals of the metals also play an important role in the interaction with H_2.

Moreover, grand canonical Monte Carlo (GCMC) simulations were used to compute hydrogen uptakes in MIL-88s at the temperatures of 77 K and 298 K and the pressures up to 100 bar. For Fe based-MIL-88 series, we found that MIL-88D is very promising for the gravimetric hydrogen storage (absolute/excess uptakes = 5.15/4.03 wt% at 77 K and 0.69/0.23 wt% at 298 K), but MIL-88A is the best alternative for the absolute/excess volumetric

hydrogen storage with 50.69/44.32 g/L at 77 K and 6.97/2.49 g/L at 298 K. Via this research, scandium (Sc) was also found as the best transition metal element for the replacement of Fe in MIL-88A for the hydrogen storage, in which absolute/excess uptakes are 5.30/4.63 wt% at 77 K and 0.72/0.29 wt% at 298 K for gravimetric uptakes; 51.99/45.51 g/L at 77 K and 7.08/2.83 g/L at 298 K for volumetric uptakes. The hydrogen storage capacity is the decrease in the order: Sc-, Ti-, V-, Cr-, Mn-, Fe-, and Co-MIL-88A. The calculations showed that the results are comparable to the best MOFs for the hydrogen storage up to date. The results also elucidated that the gravimetric hydrogen uptakes depend on the special surface area and pore volume of the MIL-88s. These important structural features, if properly improved, lead to an increase in the capability of hydrogen storage in MIL-88s.

INTRODUCTION

1. Motivation for study

Hydrogen gas (H_2) is an attractive source for potential clean energy because it is most abundant in the universe as part of water, hydrocarbons, and biomass, *etc.* Moreover, using energy from the H_2 gas does not emit the CO_2 gas and not pollute the environment like the burning of fossil fuels. In recent years, the material-based hydrogen storage is expected to provide the safe, efficient and commercial solution for hydrogen storage in both transportation and stationary applications. However, in order to use the hydrogen energy source, most commonly used in the fuel cell technology, it is necessary to develop a comprehensive system of generating production, storage, delivery, and fuel cell technologies for hydrogen. In which, the H_2 gas storage has been challenging because of its low density. Therefore, seeking advanced storage materials plays a vital role in the success of hydrogen energy technology. The 2020 targets for the H_2 storage set by the U.S. Department of Energy (DOE) are 1.8 kWh/kg (55 mg H_2 per gram of the (MOF+H_2) system, *i.e.* 5.5 wt% H_2) for gravimetric storage capacity and 1.3 kWh/L (40 g H_2/L) for volumetric storage under moderate temperatures and pressures (Hwang & Varma 2014). Various materials have been studied for hydrogen storage such as metal hydrides, carbon-based materials, zeolites, zeolitic imidazolate frameworks (ZIFs), covalent organic frameworks (COFs), and MOFs. Among them, MOFs having the ultrahigh surface area, high porosity and controllable structural characteristics are the most promising candidates for the commercial hydrogen storage. Although thousands of MOFs have been successfully synthesized, only a few of them have been tested for hydrogen storage. MIL-88 series (hereafter denoted as MIL-88s, where s = A, B, C and D; MIL = Materials from Institut Lavoisier) has attracted my attention due to consisting of the coordinatively unsaturated metal sites (CUS), one of the most effective strategic solutions for improving the gas storage capacity. Furthermore, MIL-88s structures have high flexibility and thermal stability; and hence, they are expected to be good candidates for long-term hydrogen storage. Although MIL-88s has been assessed for catalyst (Wang et al. 2016), NO adsorption (McKinlay et al. 2013), and CO_2 capture (Wongsakulphasatch et al. 2016), they has not yet been explored for hydrogen storage.

In this dissertation, vdW-DFT calculations are utilized to examine favourable adsorption sites of H_2 in the MIL-88s via the adsorption energy. The interaction of the H_2 molecule with MIL-88 series is also clarified through electronic structure properties such as the electronic density of states (DOS), charge density difference (CDD), Bader charge, overlapping DOS between the gas molecule and MOF, and the overlapping of the wave functions. Besides,

grand canonical Monte Carlo (GCMC) simulations are used to assess quantitatively the H_2 storage capability via the H_2 adsorption isotherms of MIL-88s and the strength of the H_2@MOF interaction through the isosteric heat of adsorption.

2. Structure of PhD dissertation

The structure of this dissertation consists of 6 chapters and the supporting contents, described as follows

- **Introduction:** introduce the motivation and the outline of this dissertation.
- **Chapter 1: Literature review of metal-organic frameworks:** an overview of MOFs, main applications of MOFs, the overview of experimental and computational research methods in the literature are introduced.
- **Chapter 2: Computational methods:** introducing the theory of the computational methods that are density functional theory (DFT) using revPBE functional and Grand canonical Monte Carlo (GCMC) simulations. We also provide computational details for the concerns of this dissertation.
- **Chapter 3: Hydrogen gas adsorption in Co-MIL-88A:** the hydrogen adsorption of Co-MIL-88A is studied and the physical origin for the interaction between H_2 and Co-MIL-88A is explained. Firstly, searching for the most favourable adsorption sites of H_2 is performed via computing the adsorption energy, and then the electronic properties are analyzed based on vdW-DFT calculations. Finally, hydrogen adsorption isotherms of the Co-MIL-88A are computed by GCMC simulations.
- **Chapter 4: Hydrogen storage in MIL-88 series:** MIL-88 series including MIL-88A, B, C, and D is considered for hydrogen storage capacity. GCMC simulations quantitatively assess the H_2 uptakes of the MIL-88s sorbents via the H_2 adsorption isotherms at 77 K and 298 K with the pressures below 100 bar using the GCMC simulations. The vdW-DF calculations elucidate the interaction between the H_2 molecule and the MIL-88s.
- **Chapter 5: Effects of metal substitution in MIL-88A on hydrogen adsorption:** performing to evaluate hydrogen storage capacity of MIL-88A and the effects of transition metal substitution on H_2 adsorption in M-MIL-88A (M is Sc, Ti, V, Cr, Mn, Fe, and Co). Moreover, the adsorption energies of H_2 with M-MIL-88A at the side-on and end-on adsorption configurations closing to the metal centers are calculated by the vdW-DF approach to search the most stable configurations. Besides, electronic properties are also clarified for the stable adsorption configurations. Via the GCMC simulations, the hydrogen adsorption isotherms at 77 K and 298 K and the isosteric heats of hydrogen adsorption in M-MIL-88A series are also studied.
- **Chapter 6: Conclusions and outlook:** highlighting the main findings, scientific contributions, and give an outlook for this topic in the near future.

CHAPTER 1: LITERATURE REVIEW OF METAL-ORGANIC FRAMEWORKS

1.1. General overview of metal-organic frameworks

1.1.1. Definition of metal-organic frameworks

MOFs are the compounds constructed by two main components that are inorganic metal ions/clusters and organic ligands/linkers (Zhou et al. 2012). Figure 1.1 shows a simple topology of MOF consisting of metal nodes connected to organic linkers to form a three-dimensional (3D) framework.

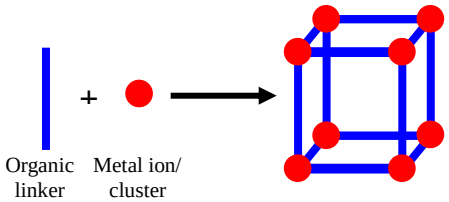

Figure 1.1. Simple topology of MOFs.

1.1.2. Structural aspects of MOFs

1.1.2.1. Primary building units

The metal ions connecting with the organic ligands are basic primary units resulting in the porous 3D structure of MOFs. Therefore, metal ions and organic compounds are used as the primary building units (PBUs) of MOFs.

1.1.2.2. Secondary building units

Organic ligands of MOFs are connected via metal-oxygen-carbon clusters, instead of metal ions alone. These metal-oxygen-carbon clusters are called as secondary building units (SBUs). SBUs have intrinsic geometric properties, facilitating MOF's topology.

1.1.3. History of MOFs

During the last two decades, MOFs continuously set new records in terms of specific surface area (SSA), pore volume, and gas storage capacities. MOF-177 and MOF-210 are the two of MOFs which have been technically tested for H_2 storage and CO_2 capture with exceptionally high storage capacity at 77 K and relatively low pressure (≤ 100 bar). Reported to date, NU-109 and NU-110 exhibited the highest experimental BET surface area (S_{BET}) with 7000 m^2/g and 7140 m^2/g, respectively (Farha et al. 2012). Nowadays, thousands of different types of MOFs have been known and they have been continuously developing further. In general, SSA of MOFs is much larger than the surface area of other traditional inorganic materials such as zeolites, silicas (< 1000 m^2/g), and activated carbons (< 2000 m^2/g). Pore volume is also one of the most important characteristics affecting the adsorption capacity of porous materials.

1.1.4. Nomenclature

MOFs have been named either by a sequence of isoreticular synthesis, the sequential number of synthesis/chronological order of discovery or the initials of the Institution or Laboratory where they were first synthesized.

1.1.5. Current research of MOFs in Vietnam

In Vietnam, MOFs have been studied by several research groups, e.g., the experimental research group of Nam T. S. Phan (Faculty of Chemical Engineering, HCMC University of Technology), the Center for Innovative Materials and Architectures (INOMAR), VNU-HCM; Institute of Materials Science and Institute of Chemistry, Vietnam Academy of Science and Technology (VAST), Ha Noi; Institute of Chemical Technology, Vietnam Academy of Science and Technology; University of Sciences, Hue University, University of Science, VNU-HCM and so on. In addition to our computational research group, the groups of Dr. Nguyen-Nguyen Pham-Tran (Faculty of Chemistry, University of Science, VNU-HCM) and Dr. Hung M. Le (INOMAR) also have studied the MOFs by DFT and GCMC simulations.

1.2. Major applications of MOFs

Due to the flexible combination of organic and inorganic components, MOFs offer many outstanding structural characteristics such as exceptionally large surface areas, high pore volume, ultrahigh porosity, complete exposure of metal sites, and high mobility of guest species in the nanopores of frameworks. MOFs can be widely used for many applications such as catalysis, gas capture and storage, gas separation/purification, sensing, biological application, and semiconductors, *etc*.

In 2003, hydrogen storage was firstly investigated on MOF-5 with the uptakes of 4.5 wt% (78 K, 0.8 bar) and 1.0 wt% (298 K, 20 bar) (Rosi et al. 2003). This report has attracted much attention and opened a new research direction for computational simulations. Assessment of hydrogen storage in the MOF was firstly calculated in 2004 using GCMC simulations and UFF by Ganz group (Sagara et al. 2004). Up to now, the experimental record in the highest total (or absolute) H_2 uptake was found in MOF-210 with 17.6 wt% at 77 K and 80 bar (excess uptake = 8.6 wt%) (Furukawa et al. 2010). The highest excess H_2 uptake is of NU-100 with 9.95 wt% at 56 bar and 77 K (absolute uptake = 16.4 wt% at 70 bar) (Farha et al. 2010). Due to the weak H_2@MOF interaction and the low isosteric heat of H_2 adsorption (typically 4 – 13 kJ/mol), hydrogen uptakes of MOFs exhibited significant only at cryogenic temperature and quite low at room temperatures, the highest *ca*. 1.0 wt% for excess uptake and 2.3 wt% for absolute uptake. Although none of MOFs has reached the DOE targets at room temperatures, they contain several key characteristics that are expected to improve and ultimately produce new MOFs with exceptional

properties for hydrogen storage. Various solutions for improving the storage capacity at ambient temperature have been suggested. One of the most effective solutions is using the MOF containing CUS. In recent years, the supports from computer simulations allow predicting and designing new MOFs that can significantly improve hydrogen uptakes.

1.3. Overview of synthesis and research methods for MOFs

1.3.1. Synthesis methods for MOFs

MOFs are synthesized by the combination of organic ligands and metal salts in solvothermal reactions at relatively low temperatures (below 300°C). The reactants are mixed in the boiling and polar solvents which are water, dialkyl formamide, dimethyl sulfoxide, acetonitrile and so forth.

1.3.2. Theoretical studies

Nowadays, theoretical studies have been proven to be useful to help explaining what is happening in the experiments and reduce expensive, difficult and time consuming experimental studies. The application of computational methods to investigate H_2 adsorption properties of MOFs has been identified as crucial to the direction of finding an efficient solution to the hydrogen storage problem, see Ref. (Tylianakis et al. 2011) and references therein.

1.4. MIL-88s for hydrogen storage

Although thousands of MOF structures have been synthesized, only a few of them were evaluated for hydrogen storage, especially at ambient temperatures and low pressures. Among them, I pay attention to the MIL-88 series which has been studied for many potential applications. MIL-88 series is interested in hydrogen storage because of the following reasons:

- MIL-88 series has very high flexibility and stability, which can avoid being collapsed if it is exposed to a humid environment.
- MIL-88s containing exposed metal sites is one of the most effective solutions to improve gas adsorption.
- So far, MIL-88 series has not yet been evaluated for H_2 storage.

In this dissertation, MIL-88 series is investigated for the first time for H_2 storage by using the most up-to-date and reliable version of computational methods which are the dispersion-corrected version of density functional theory calculations in combination with grand canonical Monte Carlo simulations. Through analysis of the results, the capability of utilizing MIL-88 series for hydrogen storage can be gauged. Moreover, the scientific results are new and become important references for experimental researches, contributing to the field of hydrogen storage for the energy application.

CHAPTER 2: COMPUTATIONAL METHODS

2.1. Density functional theory calculations

2.1.1. The Schrödinger equation

Many-body problem is a vast physical one relating to the properties of microscopic systems made of a large number of interacting particles, covered by the time-dependent Schrödinger equation in a general form as follows:

$$\hat{H}\Psi(\vec{r},\vec{R},t) = E\Psi(\vec{r},\vec{R},t), \tag{2.1}$$

where E is the total energy and Ψ is the wave function, $\hat{H}$ is the Hamiltonian operator is given by

$$\hat{H} = \hat{T}_e + \hat{T}_N + \hat{V}_{ee}(\vec{r}) + \hat{V}_{NN}(\vec{R}) + \hat{V}_{Ne}(\vec{r},\vec{R}), \tag{2.2}$$

in which $\vec{r}$ stands for a set of $\left\{\vec{r}_1,\vec{r}_2,\ldots,\vec{r}_{N_e}\right\}$ that are the coordinates of N_e electrons, and $\vec{R} = \left\{\vec{R}_1,\vec{R}_2,\ldots,\vec{R}_N\right\}$ that are the coordinates of N nuclei.

Substituting for $\hat{H}$ in (2.1) by using (2.2), we obtain the following equation

$$\left[\hat{T}_e + \hat{T}_N + \hat{V}_{\text{ee}}(\vec{r}) + \hat{V}_{NN}(\vec{R}) + \hat{V}_{Ne}(\vec{r},\vec{R})\right]\Psi(\vec{r},\vec{R},t) = E\Psi(\vec{r},\vec{R},t). \tag{2.3}$$

Basically, equation (2.3) must be solved to appropriate boundary conditions, decay to zero at infinity for an atom or molecule or obeying appropriate periodic boundary conditions for a regular infinite solid. Solving (2.3) will obtain the energy value E, the wave function Ψ, and then the probability distribution function $|\Psi|^2$. However, this equation is very difficult to solve when N is enough large. The system even containing more than one nucleus with one electron also demands highly time for calculation. Therefore, it is necessary to use Born-Oppenheimer and adiabatic approximations to separate this equation into Schrödinger equations for electrons and nuclei.

2.1.2. Born-Oppenheimer and adiabatic approximations

Because the mass of the nuclei is much larger than the mass of the electrons, the nuclei move much slower than the electrons. Therefore, nuclei can be considered stationary in the electronic structure calculation. It means that the movement of nuclei is assumed not to induce excitations in the electronic system. The nuclei are treated as fixed points in space. Applying these approximations, we can separate the wave function of the system as follows

$$\Psi(\vec{r},\vec{R},t) = \Phi(\vec{r},\vec{R})\xi(\vec{R},t), \tag{2.4}$$

where $\Phi(\vec{r},\vec{R})$ and $\xi(\vec{R},t)$ are wave functions of electrons and nuclei.

Based on these approximations, the Schrödinger equation can be separated into two Schrödinger equations of electrons and nuclei

$$\hat{H}_e \Phi\left(\vec{r},\vec{R}\right) = E\left(\vec{R}\right)\Phi\left(\vec{r},\vec{R}\right) \tag{2.5}$$

and

$$\left[\hat{T}_N + \hat{V}_{NN}\left(\vec{R}\right) + \hat{H}_e\left(\vec{R}\right)\right]\xi\left(\vec{R},t\right) = E_N \xi\left(\vec{R},t\right). \tag{2.6}$$

Here $\hat{H}_e = \hat{T}_e + \hat{V}_{\text{ee}} + \hat{V}_{Ne}$ is the Hamiltonian of electrons in the system corresponding to external potential $\hat{V}_{Ne}$ describing nucleus-electron interactions; $\varepsilon(\vec{R})$ is the energy of electrons, which depends parametrically on the ionic positions. The electronic energy is calculated by solving the time-independent Schrödinger equation (2.5) for the fixed nuclear configuration. One of the most popular and effective methods is density functional theory (DFT).

2.1.3. Thomas-Fermi theory

The Thomas-Fermi model is the first density functional theory based on the uniform electron gas, proposed by Thomas (1927) and independently Fermi (1928) (Kohanoff 2006).

2.1.4. Hohenberg-Kohn theorems

In 1964, based on the new DFT, Hohenberg and Kohn (Hohenberg et al. 1990) showed that this principle could be generalized to any electronic system.

2.1.5. Variational principle for the ground state

The variational principle states that the energy computed from a guessed Ψ is an upper bound to the true ground-state energy E_{o}: $E[\Psi] \geq E_{\text{o}}$.

2.1.6. The Kohn-Sham equations

The Thomas-Fermi model provided the first DFT based on the uniform electron gas; however, its performance is not so good due to the poor approximation of the kinetic energy; thus, Kohn and Sham proposed a new approach in 1965 based on the ideas of Hohenberg and Kohn, described below

Supposing the non-interacting N_e-electron system is given by

$$\hat{H}_R = \sum_{i=1}^{N_e}\left[-\frac{\hbar^2}{2m_e}\nabla_i^2 + u_R\left(\vec{r}_i\right)\right], \tag{2.7}$$

where $u_R\left(\vec{r}_i\right)$ is the reference potential. The Schrödinger equation for one electron in the system of non-interacting electrons has the form:

$$\hat{H}_{KS}\varphi_i\left(\vec{r}\right) = \varepsilon_i\varphi_i\left(\vec{r}\right),\ \ \hat{H}_{KS} = -\frac{\hbar^2}{2m_e}\nabla_i^2 + u_R\left(\vec{r}_i\right). \tag{2.8}$$

The electron charge density is also determined by $\rho(\vec{r}) = \sum_{i=1}^{N_e} |\varphi_i(\vec{r})|^2$.

The reference potential is determined by

$$u_R(\vec{r}) = V_{Ne}(\vec{r}) + \int \frac{\rho(\vec{r}')}{|\vec{r} - \vec{r}'|} d\vec{r}' + \mu_{XC}[\rho(\vec{r})]. \quad (2.9)$$

Where $\mu_{XC}[\rho] = \frac{\delta E_{XC}[\rho]}{\delta \rho(\vec{r})}$, in which $E_{XC}[\rho] = E_C[\rho] + E_X[\rho]$ is the correlation and exchange energy. If $u_R(\vec{r})$ in (2.9) is determined (*i.e.* $V_{Ne}(\vec{r})$ and $\mu_{XC}[\rho(\vec{r})]$ are determined), the Kohn - Sham equation will be solved.

$$\left\{ -\frac{\hbar^2}{2m_e}\nabla^2 + V_{Ne}(\vec{r}) + \int \frac{\rho(\vec{r}')}{|\vec{r} - \vec{r}'|} d\vec{r}' + \mu_{XC}[\rho(\vec{r})] \right\} \varphi_i(\vec{r}) = \varepsilon_i \varphi_i(\vec{r}) \quad (2.10)$$

2.1.7. Self-consistent field methods

By solving the Kohn-Sham equation for a self-consistent loop (Figure 2.1), we will obtain the output density $\rho_{out}(\vec{r})$: $\rho_{out}(\vec{r}) = \sum_{i=1}^{N} |\varphi_i[\rho_{in}](\vec{r})|^2$

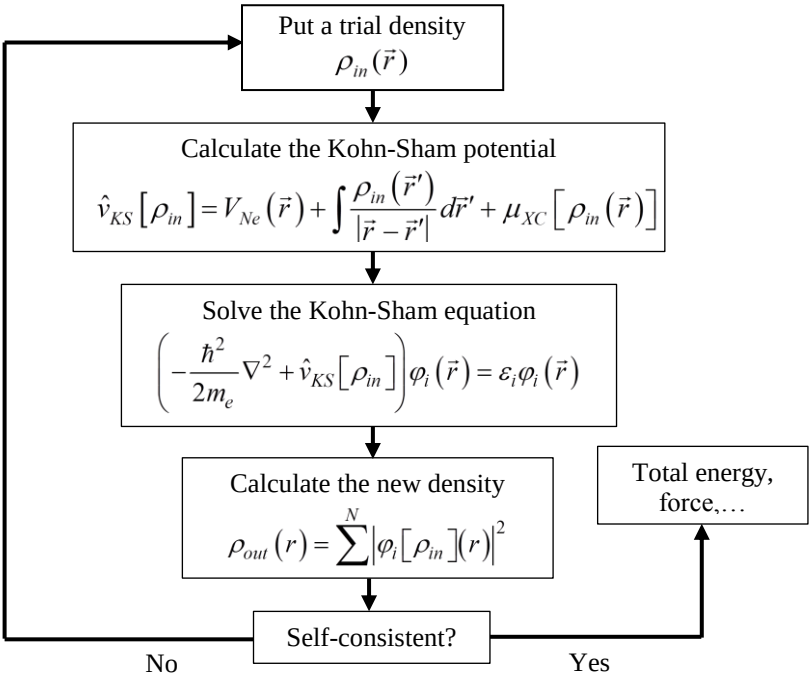

Figure 2.1. Flow chart of a self-consistent loop of the Kohn-Sham equation.

Note that $\rho_{out}(\vec{r})$ and $\rho_{in}(\vec{r})$ (or $\upsilon_{KS}[\rho_{in}]$ and $\upsilon_{KS}[\rho_{out}]$) must satisfy the self-consistent condition, *i.e.* they must be equal within a certain error limit in the energy.

2.1.8. Van der Waals density functional (vdW-DF) calculations

A proper theory for solids and molecules should take into account all types of interactions consisting of the electrostatic interactions, covalent bonds, hydrogen bonds, and van der Waals interactions (Klime et al. 2011). However, the conventional DFT with LDA or GGA cannot capture the van der Waals interactions. London dispersion interactions contribute to the stability of a wide variety of systems ranging from biomolecules to molecules adsorbed on the surface of materials. Among them, the van der Waals dispersion-corrected density functional theory (vdW-DF) method has been received great attention since it can be incorporated with the DFT framework.

2.1.9. Computational details

For the study of favourable adsorption sites and electronic structure properties, the Vienna ab initio simulation package (VASP) (Kresse & Furthmüller 1996) with vdW-DF calculations of Lundqvist et al. (Dion et al. 2004) was employed. The plane-wave basis set with the cut-off energy of 700 eV, the revBPE functional for the exchange-correlation energy, and the projector-augmented-wave method for the electron-ion interaction were used to perform the calculations. The surface Brillouin-zone integrations were performed by using the Monkhorst and Pack k-point sampling technique with the 4×4×4 grid and the Gamma point at the centre. The Methfessel-Paxton smearing of order 1 was used for the geometry relaxation with the smearing width sigma of 0.1 eV. However, the linear tetrahedron method with Blöchl corrections was employed for the calculations of total energy. For computing the favourable adsorption sites of hydrogen molecule (H_2) in the MIL-88s, we calculated the adsorption energy (E_{ads}) of H_2 in the MOF by using the equation:

$$E_{ads} = -E_b = E_{[MOF+H_2]} - \left(E_{MOF} + E_{H_2}\right), \qquad (2.11)$$

where $E_{[MOF+H_2]}$ is the total energy of a [MOF + H_2] system (*i.e.* the total energy of MIL-88A with an absorbed hydrogen molecule); E_{MOF} and E_{H_2} are the total energy of the pristine MOF, and the isolated hydrogen molecule, respectively.

2.2. Grand canonical Monte Carlo (GCMC) simulations

2.2.1. Introduction

GCMC simulations have been used to calculate the hydrogen uptake of MOFs. In this method, the number of particles in the system allowed to change

during the simulation process by random test steps such as creation, deletion, displacement or rotation so that the system reaches to the equilibrium state. The accuracy of a GCMC simulation describing the interatomic interactions between the H_2 molecule and the MOFs depends on the accuracy of the force fields, compared with the experimental data. Force fields have been employed in H_2 adsorption simulations that are generic force fields: UFF (Rappe et al. 1992), DREIDING (Mayo et al. 1990) and OPLS (optimized potential for liquid simulations) (Carlo et al. 2006).

2.2.2. Computational details

GCMC simulations were used to compute the gravimetric loadings of hydrogen gas in the MIL-88s by using the simulation package RASPA, the molecular simulation software for nanoporous materials (Dubbeldam et al. 2016). These simulations were performed in the $VT\mu$ ensembles at 77 K and 298 K, and pressures $\leq$ 100 bar. The number of equilibration cycles was 10^5 steps, followed by 3×10^5 MC steps for the random insertion, deletion, translation, and rotation of hydrogen molecules in the simulation box. The framework was kept rigid during the simulation process, while the hydrogen molecule freely moves in the MOF structure. The interaction between the H_2 gas and the atoms (C, O, H and metal) of the MOF were described through the Lennard-Jones (LJ) 6-12 potential and the electrostatic potential:

$$U\left(r_{ij}\right)=4\varepsilon_{ij}\left[\left(\frac{\sigma_{ij}}{r_{ij}}\right)^{12}-\left(\frac{\sigma_{ij}}{r_{ij}}\right)^{6}\right]+\frac{1}{4\pi\varepsilon_{o}}\frac{q_i q_j}{r_{ij}}, \qquad (2.12)$$

where U is the potential energy between a pair of atoms i and j at a distance r_{ij}; ε_o is the dielectric constant; q_i is the partial charge of atom i obtained from the DDEC atomic net charge calculation based on the DFT method. The parameters ε_{ij} and σ_{ij} are the LJ potential well depth and diameter. The LJ interaction is neglected beyond the cutoff radius of 12.8 Å.

Partial charges for the atoms in MIL-88s were computed by DDEC method. These point charges were assigned to atomic sites to compute the electrostatic interaction. This interaction was handled using the Ewald summation technique with the cutoff radius of 12 Å. For the hydrogen molecule, a single LJ interaction site model at the centre of mass (H_{com}) was used with the LJ parameters were taken from the TraPPE force field (Levesque et al. 2002).

CHAPTER 3: HYDROGEN ADSORPTION IN Co-MIL-88A

3.1. Optimization of Co-MIL-88A unit cell

The MIL-88A was designed with the chemical formula $[\{M_3O(\text{-}O_2C\text{-}C_2H_2\text{-}CO_2\text{-})_3\}]_n$ having a 3D hexagonal structure consisting of the trimers of metal octahedra linked to the fumarate ligands, where n is the number of chemical formula units. Figure 3.1 shows the structure of the unit cell of Co-based MIL-88A with $n = 2$. The cell parameters of the unit cell are $a = b \neq c$ and the angles $\alpha = \beta = 90°$, $\gamma = 120°$. After the primary unit cell of Co-MIL-88A was designed, the geometry optimization for Co-MIL-88A was performed for its volume and ionic positions that were fully relaxed by using vdW-DF (Dion et al. 2004). By fitting based on the Murnaghan equation of state (EOS) (Murnaghan 1951), the optimized lattice constants for the unit cell of Co-MIL-88A are $a = b = 11.222$ Å and $c = 14.719$ Å, resulting in a volume of 1605.34 Å^3.

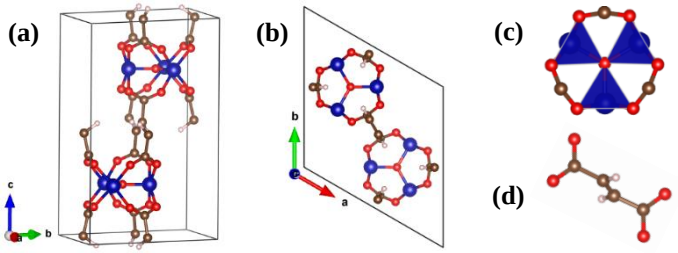

Figure 3.1. The unit cell of Co-MIL-88A: (a) side view, (b) top view of the unit cell, (c) μ_3-O-centered trimer of Co metals, and (d) fumarate ligand of MIL-88A.

3.2. Searching stable hydrogen adsorption sites

When obtaining the optimized Co-MIL-88A unit cell, a hydrogen molecule (H_2) is loaded into the structure at many different sites, and then geometry optimization is performed and the adsorption energy of H_2 in Co-MIL-88A is calculated. The results are listed in Table 3.1 together with the average bond length of H_2 to the closest atoms of the MOF.

Table 3.1. The adsorption energy (E_{ads}) for the favourable adsorption sites. The average distance between H_2 and the reference atoms of the MOF (d_{H_2-A}) and the Bader point charge of H_2 (q_{H_2}).

Sites	E_{ads} (kJ/mol)	E_b (kJ/mol)	d_{H_2-A} (Å)	q_{H_2} (e)
Hollow	-13.72	13.72	3.20	-0.0002
Ligand	-10.76	10.76	3.41	-0.0006
Metal (side-on)	-10.61	10.61	3.14	-0.0038
Metal (end-on)	-6.50	6.50	3.15	-0.0006

The results show the favourable adsorption site is in the order of hollow > ligand > metal side-on > metal end-on. The most favourable adsorption of H_2 is at the hollow site between two COO^- groups linked to Co atoms. At this position, the H_2-MIL-88A binding energy is 13.72 kJ/mol. The reason for the stronger adsorption of H_2 on the organic ligand compared to the metal site may be due to the relatively short fumarate bridges. Thereby, the metal and oxygen atoms may interact with the H_2 located at the hollow and ligand sites. For the H_2 adsorbed end-on configuration on the metal site, the binding energy of this configuration is the smallest compared with that of the others.

For deeper insights into the H_2@MIL-88A interaction, the electronic properties are analyzed through CDD and DOS. The CDD between H_2 and Co-MIL-88A is shown in Figure 3.2. For the hollow, ligand, and side-on (metal) configurations, the H_2 molecule interacts with the Co-MIL-88A through its bonding (σ) state, while the anti-bonding (σ^*) state of H_2 interacts with Co-MIL-88A at the end-on site. The charge exchange cloud of the H_2 molecule closest to the MOF shows a charge gain for the cases of the H_2 molecule adsorbed on the ligand, side-on, and end-on sites via the yellow clouds; however, it shows a charge donation for the hollow site with the most favourable adsorption (cyan cloud). The hollow configuration (Figure 3.2a) has the largest charge exchange cloud due to the strongest interaction of H_2 with the MOF, while the end-on configuration on the metal (Figure 3.2b) has the smallest charge exchange cloud because of the weakest interaction.

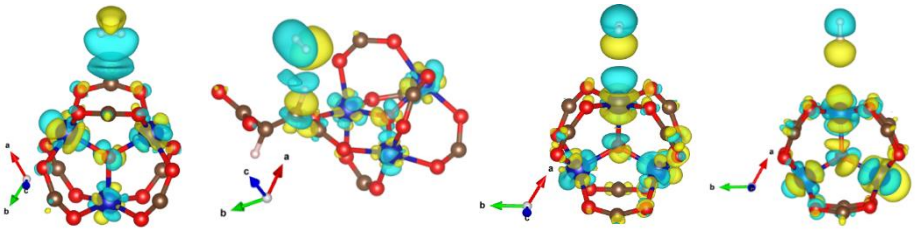

a) Hollow b) Ligand c) Metal (side-on) d) Metal (end-on)

Figure 3.2. CDD for the favourable adsorption configurations of H_2 in Co-MIL-88A. The orbitals are drawn at an isosurface value of 0.0002 *e*/Bohr^3. Yellow (positive) and cyan (negative) clouds indicate charge gain and loss.

The Bader charge exchange of H_2 in Co-MIL-88A is also listed in Table 3.1. The result shows that the Bader charge of the adsorbed H_2 is very small and within the error of the charge calculation of 0.0005 *e*. Therefore, it can be concluded that there is no significant charge transfer between H_2 and Co-MIL-88A because of the weak physisorption of the H_2 molecule in the MOF.

A deeper understanding of the MOF – H_2 interaction can be exposed through the overlapping of DOS curves describing the interaction between H_2 and Co atoms of the MIL-88A. Figure 3.3 indicates the bonding state (σ) of H_2

overlaps with the *d* orbitals of the Co atoms. For the hollow, the ligand, and the metal side-on configurations, the d_{xy}, $d_{x^2-y^2}$ and d_{z^2} orbitals of the metal atoms mainly contribute to the interaction with H_2, while it is the d_{z^2} orbital for the metal end-on configuration. The *s* orbital of the Co atoms of the MOF also contributes to the interaction with H_2 but most substantially for the most favourable H_2 adsorption configuration, on the hollow site. Although the H_2 molecule at the hollow site is far away from the nearest Co atoms with the average distance of 4.15 Å, the interaction of the H_2 with the Co atoms is still possible through the indirect interaction with the oxygen atoms in the outer space of the metal oxide. Figure 3.4 elucidates the interaction between H_2 and Co atoms via the real-space wave functions (Feenstra et al. 2013), showing that there is an overlapping between the wave function of the H atoms of the H_2 molecule and that of the Co atoms.

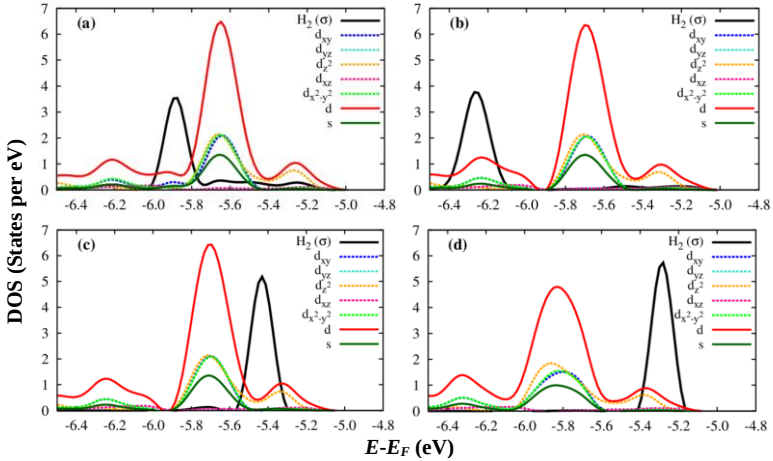

Figure 3.3. DOS of the hydrogen molecule and the *s* and *d* orbitals of the Co atoms of the Co-MIL-88A at the sites: hollow (a), ligand (b), metal side-on (c), and metal end-on (d).

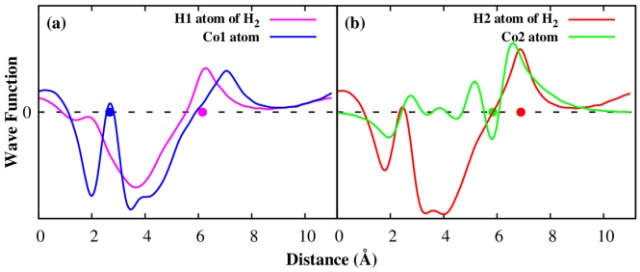

Figure 3.4. The real part of the wave functions of the H atom of H_2 and the Co atom of MIL-88A along the *x*-direction. The dots denote for the position of the atoms.

Remarkably, the H_2@Co-MIL-88A interaction strength is quantitatively assessed by calculating an overlapping of DOS (Hoffmann 1988), which is the overlap area between the DOS of the adsorbed H_2 and the DOS of the atomic orbitals of Co-MIL-88A. The calculated results are listed in column 7 of Table 3.2. It indicates that overlapping DOS correlates with the binding energy, *i.e.*, the larger the overlapping of DOS is, the stronger the binding strength becomes. The last column of Table 3.2 also shows that the more stable the H_2 adsorption configuration becomes, the lower the peak height of the H_2 DOS is, *i.e.* the DOS area of the H_2 molecule adsorbed in Co-MIL-88A decreases versus the increase in the H_2@Co-MIL-88A interaction. Table 3.2 shows that the overlapping of the H_2 DOS with the *s*, *d* orbitals of Co atoms and the *p* orbital of the μ_3-O atoms monotonically increase in the order: the metal end-on, the metal side-on, the ligand, the hollow site. In general, the inner atoms of the trimers such as Co and μ_3-O become more and more important for stabilizing the H_2 adsorption.

Table 3.2. Overlapping DOS between the DOS of the adsorbed hydrogen molecule with the DOS of different components of Co-MIL-88A.

Sites	*d* orbital of Co	*s* orbital of Co	*s* and *d* orbitals of Co	*p* orbital of μ_3-O atoms	Total *p* orbital of all atoms	Total DOS of all atoms	Area of H_2 DOS
Hollow	0.750	0.378	1.128	0.793	1.277	2.405	0.7050
Ligand	0.704	0.180	0.884	0.731	1.400	2.284	0.7052
Metal side-on	0.376	0.081	0.457	0.250	1.433	1.890	0.7358
Metal end-on	0.258	0.017	0.275	0.049	1.488	1.763	0.7836

3.3. Adsorption isotherms of hydrogen in Co-MIL-88A

In order to determine hydrogen uptakes in Co-MIL-88A, the point charges of the atoms (Co, C, O, and H) are computed by the DDEC method based on DFT calculations combining to the LJ parameters are taken in generic force fields (UFF) for MOFs. For assessment of the adsorption capacity of H_2 in Co-MIL-88A at temperatures of 77 K and 298 K and pressures up to 100 bar, the average amount of absolute and excess uptakes was computed. Typically, for physisorption system, the scope of the isotherms in Figure 3.5 represents type-I adsorption isotherm in the IUPAC classification (Sing et al. 1982). Figure 3.5a shows that the H_2 adsorption isotherms at 77 K increase sharply below 5 bar and achieves the maximum value of about 4.0 wt% at 12 bar for the excess uptake but still increases slightly for the absolute uptake until 100 bar and reaches the value of 4.6 wt%. From these results, we see the H_2 uptake in Co-MIL-88A at the cryogenic temperature (77 K) is moderate compared with that of the best MOFs reported up to now, see the above section for the overview of

hydrogen storage. The sudden increase of the isotherm at low pressures implies that the storage is mainly based on the adsorption of H_2 in Co-MIL-88A.

The H_2 adsorption isotherms at 298 K (Figure 3.5b) increase fairly close to a linear function of the pressure, but are not saturated at the highest pressure of 100 bar. This result implies that the Co-MIL-88A is very stable and suitable for hydrogen storage at high pressures. The maximum value for the absolute and excess gravimetric uptakes at 298 K and 100 bar is 0.63 and 0.22 wt% (*i.e.* 3.15 and 1.10 mmol/g or 70.05 and 24.46 cm^3/g), respectively. The absolute hydrogen storage capacity is comparable to the experimental data obtained for the best MOFs up to date at the standard condition of 298 K and 100 bar.

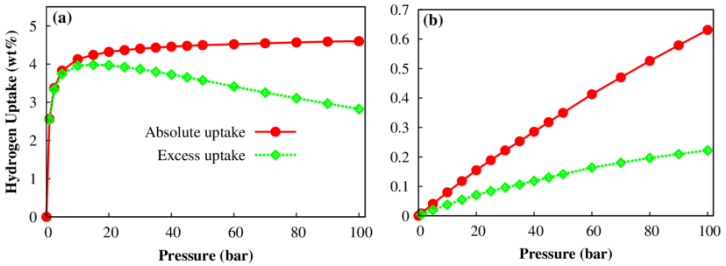

Figure 3.5. Absolute (red solid line) and excess (blue dash line) adsorption isotherms for the Co-MIL-88A at (a) 77 K and (b) 298 K.

Figure 3.6 shows the visualization of hydrogen molecules in Co-MIL-88A. The result shows that the H_2 molecules are more concentrated around the hollow than around the ligand and the metal sites, which means that the hollow site is the most favourable adsorption site of the hydrogen gas, as illustrated in DFT calculations. These results proved that the generic force field for MOFs used in could qualitatively reproduce the observation of the density functional theory results.

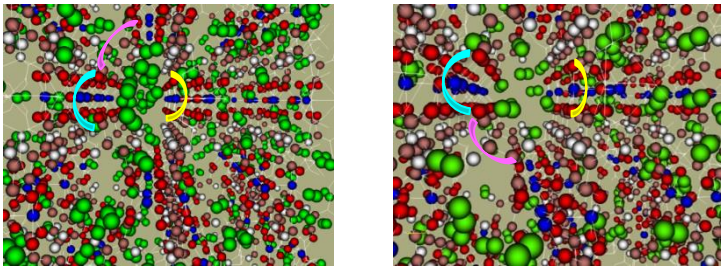

a) At 77 K, 0.1 bar b) At 298 K, 10 bar

Figure 3.6. The density of the adsorbed hydrogen molecules in the Co-MIL-88A. The blue, red, brown, white balls represent the cobalt, oxygen, carbon, and hydrogen atoms of MOF, respectively. Each pair of green balls represents an adsorbed hydrogen molecule. The cyan, pink and yellow bands refer to the hollow, ligand and metal sites, respectively.

CHAPTER 4: HYDROGEN STORAGE IN MIL-88 SERIES

4.1. Geometry optimization of MIL-88 series

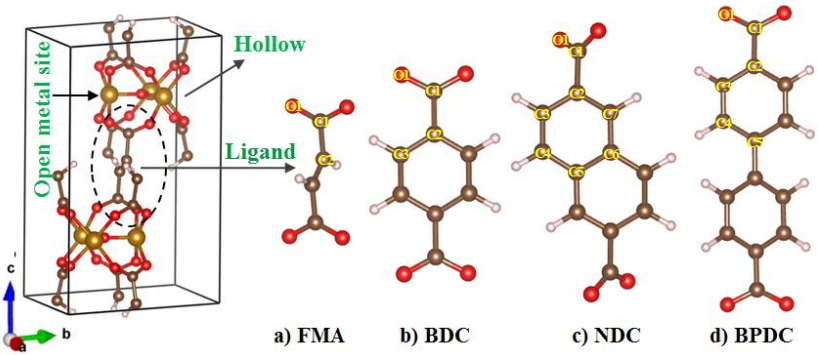

Figure 4.1. The structure of MIL-88s with ligands: FMA (a), BDC (b), NDC (c), BPDC (d).

Figure 4.1 presents the unit cell of MIL-88s with the chemical formula $\left[\left\{Fe_3O(-L-)_3\right\}\right]_2$, where L = OOC–$C_2H_2$–COO (FMA), OOC–$C_6H_4$–COO (BDC), OOC–$C_{10}H_6$–COO (NDC), OOC–$C_{12}H_8$–COO (BPDC). Figure 4.1(a–d) shows the structure of these ligands. The parameters for the unit cell of the MIL-88A, B, C, and D fitted by Murnaghan EOS is listed in Table 4.1.

Table 4.1. Cell parameters of the of the hexagonal MIL-88s compared to the data in Ref. (Surble et al. 2006).

Cell parameters	MIL-88s (fitted by Murnaghan EOS)				MIL-88s (Surble et al. 2006)			
	A	B	C	D	A	B	C	D
$a = b$ (Å)	11.22	11.11	10.21	12.04	11.18	11.05	10.22	12.05
c (Å)	14.86	19.12	23.35	27.67	14.68	18.99	23.60	27.50
V (Å^3)	1619	2043	2108	3463	1589	2008	2135	3458

4.2. Isotherms and isosteric heats of hydrogen adsorption

The adsorption capability of hydrogen in MIL-88s is also assessed based on the adsorption isotherms 77 K and 298 K, and the pressures up to 100 bar. The steep rise in the absolute and excess gravimetric H_2 adsorption isotherms at 77 K in the low-pressure range (under 10 bar) (Figure 4.2a) shows that the H_2 adsorption in MIL-88s is mainly based on the physisorption. The excess H_2 adsorption isotherms of MIL-88A, B, C, and D obtain the maximum values corresponding to 4.06 wt% (at 15 bar), 3.56 wt% (at 15 bar), 1.72 wt% (at 7.5 bar), and 4.03 wt% (at 22.5 bar) (Table 4.2). While, the absolute H_2 adsorption isotherms still increase slightly up to 100 bar and achieve the maximum values 4.66, 4.12, 1.87, and 5.15 wt% for MIL-88A, B, C, and D, respectively. The

results showed the gravimetric H_2 uptake of MIL-88D ≈ MIL-88A > MIL-88B > MIL-88C for the excess uptake and MIL-88D > MIL-88A > MIL-88B > MIL-88C for the absolute uptake. Except for MIL-88C that has low hydrogen storage capacity, the remaining structures show the gravimetric H_2 uptakes are comparable to the best MOFs evaluated for H_2 storage up to now (Table 4.2).

At 298 K, the H_2 adsorption isotherms increase linearly under pressure and remain unsaturated when the pressure is up to 100 bar (Figure 4.2b). This behaviour implies that MIL-88s is stable, thus they are suitable for the H_2 storage at high pressures. The maximum absolute H_2 uptakes at 100 bar are corresponding to 0.64, 0.58, 0.31, and 0.69 wt% for MIL-88A, B, C, and D. This result indicates the order of the H_2 adsorption in MIL-88s at 298 K is similar to that at 77 K. It is noteworthy that the excess H_2 uptakes at 298 K are the same for MIL-88A, B, and D (with the maximum value of 0.23 wt%) and they are greater than that for MIL-88C (with 0.16 wt%). These values at the room temperature are quite low compared to those of other MOF candidates evaluated highly for hydrogen storage so far, 0.36 – 2.3 wt% (see Table 4.2).

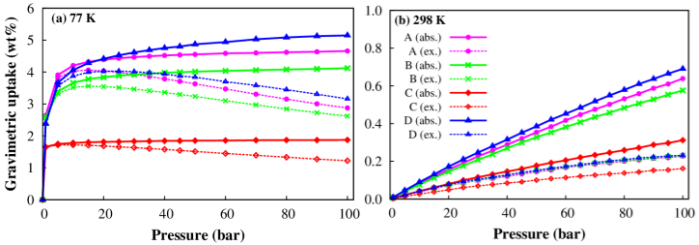

Figure 4.2. Absolute (abs.) and excess (ex.) gravimetric H_2 adsorption isotherms of the MIL-88s at (a) 77 K and (b) 298 K.

Table 4.2. The maximum absolute and excess gravimetric H_2 uptakes in MIL-88s at 77 K and 298 K, and P ≤ 100 bar. The specific surface area (SSA) and the pore volume (V_p) are also listed.

MOF	Uptake (wt%) at 77 K		Uptake (wt%) at 298 K, 100 bar		SSA (m^2/g)	V_p (cm^3/g)	
	Absolute (100 bar)	Excess	Absolute	Excess		This work	(Mitchell et al. 2013)
MIL-88A	4.66	4.06 (15 bar)	0.64	0.23	1067.04	0.52	
MIL-88B	4.12	3.56 (15 bar)	0.58	0.23	535.43	0.44	
MIL-88C	1.87	1.72 (7.5 bar)	0.31	0.16	21.45	0.19	
MIL-88D	5.15	4.03 (22.5 bar)	0.69	0.23	1199.82	0.58	0.47

The gravimetric uptake is an important quantity for evaluating the hydrogen storage of sorbents, it is equally necessary to access the volumetric H_2 storage, especially for onboard applications. Figure 4.3a and b show the absolute and excess volumetric H_2 adsorption isotherms at 77 K and 298 K, the pressures up to 100 bar. Surprisingly, at both 77 K and 298 K, MIL-88A achieves the highest absolute and excess volumetric H_2 adsorption amounts, followed by

MIL-88B, MIL-88D, and MIL-88C. The obtained the maximum values for the volumetric H_2 adsorption capacities are inferred and listed in Table 4.3. At 77 K, the absolute and excess volumetric storage capacities of MIL-88B are close to those of MIL-88D and they become overlap when the pressure increases to 100 bar. MIL-88C has the lowest absolute and excess volumetric H_2 storage capacities at both 77 and 298 K, similar to the low gravimetric uptakes. In general, the volumetric storage capacities of MIL-88s at 298 K are very low compared to the DOE target; however, their volumetric storage capacities at 77 K meet the target. MIL-88A achieved the absolute and excess H_2 volumetric uptakes corresponding to 50.69 g/L and 44.32 g/L surpassing the DOE target of 40 g/L. These values are noteworthy among the best MOFs for the volumetric storage of hydrogen gas, seen more details in the review paper of Suh and co-workers (Suh et al. 2012). For example, Be–MOF (Sumida et al. 2009) achieved the high absolute H_2 uptakes of 9.2 and 2.3 wt% at 77 and 298 K, respectively; however, its absolute volumetric adsorption reaches only 44 g/L at 77 K and the pressures under 100 bar (Table 4.2). Meanwhile, MIL-88A, B, and D obtain much higher volumetric uptakes, especially for MIL-88A with 50.69 g/L.

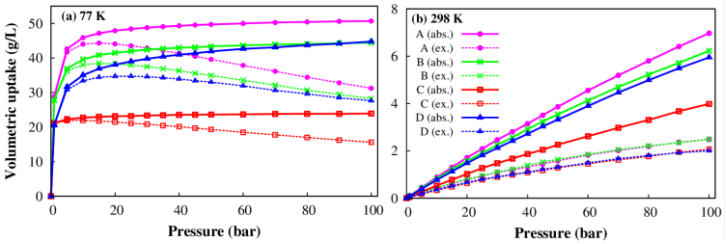

Figure 4.3. Absolute (abs.) and excess (ex.) volumetric H_2 adsorption isotherms of MIL-88s at (a) 77 K and (b) 298 K.

Table 4.3. Maximum absolute and excess volumetric H_2 uptakes of MIL-88s at 77 K and 298 K, the pressures under 100 bar.

MOF	At 77 K		At 298 K, 100 bar	
	Absolute (100 bar)	Excess	Absolute	Excess
MIL-88A	50.69	44.32 (15 bar)	6.97	2.49
MIL-88B	44.42	38.48 (15 bar)	6.23	2.49
MIL-88C	23.91	21.99 (7.5 bar)	3.98	2.07
MIL-88D	44.75	34.73 (22.5 bar)	5.95	2.00
Be-MOF (Sumida et al. 2009)	44		11	

This research also shows that the density of the H_2 molecules distributing more uniformly will help increase the amount of the sorbed hydrogen gas for MIL-88A and MIL-88D. The distribution of the H_2 adsorption also depends on SSA and V_p of the MOF, shown in columns 6 and 7 of Table 4.2. The obtained results show that the gravimetric uptakes linearly correlates with the SSA and

V_p of MIL-88s, namely MIL-88D > MIL-88A > MIL-88B > MIL-88C. Unlike the gravimetric H_2 uptakes, the volumetric H_2 storage does not linearly depend on SSA and V_p (Fairen-Jimenez et al. 2012).

4.3. The most favourable H_2 adsorption configurations

Table 4.4. Adsorption energy of H_2 in MIL-88s (E_{ads} in kJ/mol), compared to Q_{st} (in kJ/mol).

MOF	Fe metal		Hollow		Ligand		Average E_{ads} on 6 sites	$-Q_{st}$ (kJ/mol)
	Side-on	End-on	Side-on	End-on	Side-on	End-on		
MIL-88A	-12.85	-8.06	-17.19	-13.69	-10.83	-8.81	-11.91	-7.38
MIL-88B	-13.08	-11.07	-17.78	-13.78	-15.88	-14.07	-14.27	-9.69
MIL-88C	-18.32	-15.49	-17.46	-13.17	-20.64	-17.80	-17.15	-10.86
MIL-88D	-12.44	-13.81	-15.92	-11.67	-16.25	-17.53	-14.60	-10.44

The most favourable adsorption sites of H_2 in MIL-88s are searched using vdW-DF calculations. The adsorption energy (E_{ads}) is calculated for both side-on and end-on configurations on Fe metal, in the hollow between four O atoms and two Fe atoms at the inner layer, and on the ligand region. The results (Table 4.4) show that the more negative the E_{ads}, the more stable the H_2 adsorption configuration is. Remarkably, the H_2 is most favourable on the ligand for MIL-88C and D, while it is on the hollow for MIL-88A and B. The results (Table 4.4) display the good correlation between the average E_{ads} (computed over six most favourable adsorption configurations) and Q_{st} of H_2 in MIL-88s. These elucidate the average strength of the H_2@MIL-88s interaction is in the increasing order of MIL-88C, MIL-88D, MIL-88B, and MIL-88A. The DFT calculations confirm once again that the H_2@MOF interaction strength is strongest for MIL-88C, followed by MIL-88D, B, and A.

4.4. Electronic structure properties of H_2 – MIL-88s interaction

When the H_2 molecule interacts with the MIL-88s, the overlap was found between the DOS of the adsorbed H_2 and the DOS of the *d* orbital of Fe atoms, the *p* orbital of O and C atoms of MIL-88s. The results show that the DOS of the adsorbed H_2 exhibits a single peak for MIL-88A, B, and D with E_{ads} = -17.19, -17.78, and -17.53 eV, respectively, while it splits into two peaks for MIL-88C implying an enhancement in the interaction with MIL-88C leading to the most negative adsorption energy of -20.64 eV. The CDD for the most stable adsorption configurations of the H_2 molecule in MIL-88s shows that the bonding state of H_2 dominates the H_2@MIL-88s interaction, where the charge clouds extend over both hydrogen atoms of the hydrogen molecule.

CHAPTER 5: EFFECTS OF TRANSITION METAL SUBSTITUTION IN MIL-88A ON HYDROGEN ADSORPTION

5.1. Optimization of M-MIL-88A unit cell

The primary unit cell of M-MIL-88A, where M is the trivalent transition metal including Scandium (Sc), Titanium (Ti), Vanadium (V), Chromium (Cr), and Manganese (Mn) was fully optimized by using Murnaghan EOS fitting method. The result shows that the volume of M-MIL-88A decreases in the order of the transition metal series from Sc to Co, in which the volume is the largest for Sc-MOF and the smallest for Co-MOF. This is in good agreement with the trend of the optimized volume of the $M_3(BTC)_2$ structures, where SBUs contain 3 transition metals (Parkes et al. 2015).

5.2. Stable hydrogen adsorption sites

In this part, the role of metal in MIL-88A on hydrogen adsorption will be evaluated; therefore, we only focus on the [H_2 + MIL-88A] systems with the loaded H_2 closing to the metals including side-on and end-on configurations. The adsorption energies of H_2 in M-MIL-88A are listed in Table 5.1.

Table 5.1. Adsorption energies (in kJ/mol), Bader charges (in e^-) of the adsorbed H_2 in M-MIL88A compared to the isolated H_2 with (-) for the charge loss and (+) for the charge gain and other relative parameters.

Metal	Side-on			End-on				E_{ads} for M_3O cluster (Mavrandonakis et al. 2015)	E_b M-MOF-74 (Lee et al. 2015)
	d_{H_2-M}	E_{ads}	q_{H_2}	d_{H_2-M}	E_{ads}	Angle H-H-M (°)	q_{H_2}		
Sc	2.64	-14.84	-0.009	3.12	-5.72	178	0.0085	-14	
Ti	2.43	-14.92	-0.014	3.33	-4.73	180	0.0052		22
V	2.40	-17.00	-0.019	3.28	-6.65	179	0.0013	-16.7	25
Cr	2.62	-15.46	-0.013	3.19	-6.38	179	0.0032	-18	9
Mn	2.48	-15.74	-0.019	3.33	-7.20	180	0.0007		12
Fe	2.59	-12.85	-0.016	3.41	-8.06	180	0.0006		13
Co	3.14	-10.61	-0.004	3.15	-6.50	180	-0.0006		13

The results indicate that H_2 adsorption energy per H_2 molecule has the most negative value is -17.00 kJ/mol (*i.e.* E_b = 17.00 kJ/mol) for the side-on configurations of V-MIL-88A. This trend is consistent with the previous results of the groups (Mavrandonakis et al. 2015), (Lee et al. 2015), in which the MOF or the metal cluster constructed from the V element obtained the strongest H_2@MOF binding energy. The calculations show that the order of the H_2 – M-MIL-88A interaction in side-on direction is H_2@V-MIL-88A > H_2@Mn-MIL-88A > H_2@Cr-MIL-88A > H_2@Ti-MIL-88A > H_2@Sc-MIL-88A > H_2@Fe-MIL-88A > H_2@ Co-MIL-88A. For the end-on geometry, the H_2 molecule

binds linearly to the metal atom of M-MIL-88A with the H-H-M angle ~180°. The calculated H_2@M-MIL-88A binding energies for the end-on configurations, 4.73 – 8.06 kJ/mol, are much lower than those of the side-on ones (10.61 – 17.00 kJ/mol). This different adsorption can be seen clearly through the charge donation between the adsorbed H_2 and the atoms of the MIL-88A (Table 5.1). For the side-on mode, the H_2 molecule donates charge to the atoms of MOF ($q_{H_2} < 0$). In contrast, for the end-on mode, H_2 gains the charge from the atoms of M-MIL-88A. However, there is no significant charge transfer between H_2 and M-MIL-88A, especially in end-on configurations, due to the weak physisorption of the H_2 molecule. Via analyzing DOS of the adsorbed H_2 and M-MIL-88A, the results show that the interaction between H_2 and M-MIL-88A is presented not only the *d* orbital of metal but also the *p* orbitals of C and O atoms. It can be seen that the orbitals enhancing the H_2@M-MIL-88A interaction are the p_x and p_y orbitals of the O atoms, the p_z orbital of the C atoms, and d_{xy}, $d_{x^2-y^2}$ and d_{z^2} orbitals of the metals interacting with the σ state of H_2. Otherwise, for end-on modes, the interaction between the atoms of the MOF and H_2 is quite weak, where the main H_2@MOF interaction is that of the σ^* state.

5.3. Isotherms and isosteric heats of hydrogen adsorption

To further study the H_2 storage capacity in M-MIL-88A, the H_2 adsorption isotherms of M-MIL-88A were evaluated via GCMC simulations. The H_2 isotherms for M-MIL-88A series at 77K and 298 K are shown in Figure 5.1. For all structures, the H_2 adsorption isotherms at 77K (Figure 5.1a) show the steep initial increase from 0 to 10 bar in the excess hydrogen uptake and decrease at higher pressure. Besides, the hydrogen adsorption isotherms increase in the absolute uptake up to 100 bar. Sc-MIL-88A has the maximal values for absolute and excess loading, 5.30 wt% at 100 bar and 4.63 wt% at the saturated pressure of 10 bar, respectively (Table 5.2). The absolute and excess uptakes of other M-MIL-88A at 77 K, smaller than that of Sc-MIL-88A, is in the order of Ti-MIL-88A > V-MIL-88A > Cr-MIL-88A > Mn-MIL-88A > Fe-MIL-88A > Co-MIL-88A. The results show that the H_2 uptake in M-MIL-88A decreases with the decrease of ionic radius of metal cation from Sc^{3+} to Co^{3+} ion. Quite different from the isotherms at 77K, the scope of the isotherms at 298K (Figure 5.1b) is nearly linear with the increase of pressure and not yet saturate at 100 bar. This implies that M-MIL-88A series is stable. Sc-MIL-88A has the highest adsorption in both absolute and excess uptake with 0.72 wt% and 0.29 wt% at 100 bar, respectively. The uptake is in the descending order: Sc-, Ti-, V-, Cr-, Mn-, Fe-, and Co-MIL-88A. This trend agrees with the H_2

uptakes at 77 K. These H_2 uptakes in M-MIL-88A are still much smaller than the target of DOE but comparable to the high H_2 uptakes observed so far.

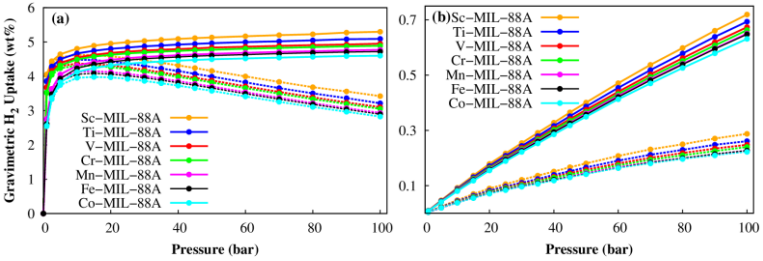

Figure 5.1. Absolute (solid) and excess (dashed) gravimetric adsorption isotherms of hydrogen in M-MIL-88A series at: (a) 77 K and (b) 298 K.

The volumetric H_2 uptakes are also evaluated via the isotherms of H_2 adsorption. The results point out that the absolute and excess volumetric H_2 uptakes of M-MIL-88A series don't depend much on the metal of MIL-88A at 77 K and 298 K. In which, the absolute and excess volumetric uptakes of hydrogen in Sc-MIL-88A is still highest with 51.99/45.51 g/L at 77 K and 7.08/2.83 g/L at 298 K. The volumetric H_2 uptakes are noteworthy.

The DFT calculations indicated that the H2@V-MIL-88A interaction between H_2 and is strongest on the side-on site of the metal. However, by GCMC simulations, the H_2 storage capacity in Sc-MIL-88A is largest. For accurate assessment of the strength of the interaction between the H_2 molecule and the MIL-88A sorbents, we calculate Q_{st}. The result shows that the order of Q_{st} of H_2 in M-MIL-88A is Sc-MIL-88A > Ti-MIL-88A > V-MIL-88A > Cr-MIL-88A > Mn-MIL-88A ≈ Fe-MIL-88A ≈ Co-MIL-88A. This tendency agrees with the gravimetric and volumetric uptakes of hydrogen. Thus, the H_2 uptakes of MIL-88A series strongly depend on the isosteric heats of H_2 adsorption. Moreover, the uptakes can correlate with the SSA and the pore volume (V_p), illustrated in chapter 4 for MIL-88A, B, C and D series.

Table 5.2. Maximum absolute and excess and gravimetric volumetric uptakes of hydrogen in M-MIL-88A at 77 K and 298 K and the pressures under 100 bar.

Compound	Gravimetric uptakes (wt%)				Volumetric uptakes (g/L)				Q_{st} (kJ/mol)
	77 K		298 K		77 K		298 K		
	Absolute	Excess	Absolute	Excess	Absolute	Excess	Absolute	Excess	
Sc-MIL-88A	5.30	4.63	0.72	0.29	51.99	45.51	7.08	2.83	9.85
Ti-MIL-88A	5.09	4.49	0.69	0.26	51.11	45.02	6.97	2.62	8.55
V-MIL-88A	4.95	4.37	0.67	0.25	50.87	44.96	6.93	2.55	8.03
Cr-MIL-88A	4.89	4.32	0.66	0.24	50.71	44.83	6.89	2.49	7.70
Mn-MIL-88A	4.77	4.15	0.65	0.23	50.64	44.03	6.90	2.41	7.26
Fe-MIL-88A	4.66	4.06	0.64	0.23	50.69	44.32	6.97	2.49	7.38
Co-MIL-88A	4.60	4.00	0.63	0.22	50.57	43.78	6.94	2.44	7.35

CHAPTER 6: CONCLUSIONS

6.1. The main findings

The DFT results showed that the most favourable adsorption of H_2 occurs at the hollow sites with the side-on configuration in MIL-88A and B, and the ligand sites in MIL-88C and D. It was found that the H_2@MIL-88s interaction was dominated by the bonding state of the H_2 molecule and the *p* orbitals of the O and C atoms in MIL-88s. For MIL-88A and B, the *d* orbitals of metals also play an important role in the interaction with the H_2 molecule, which explains the reason why the hollow site nearby the metals of MIL-88A and B becomes the preferred adsorption site.

GCMC simulations indicated that MIL-88D is the best choice among MIL-88 series to store the hydrogen gas in gravimetric capacity. The highest absolute and excess gravimetric H_2 uptakes are 5.15 wt% (100 bar), 4.03 wt% (25 bar) at 77 K and 0.69 wt%, 0.23 wt% at 100 bar and 298 K. These results are comparable with the best MOFs for hydrogen storage capacity up to date. Surprisingly, for volumetric H_2 storage, despite the lower gravimetric H_2 storage, MIL-88A achieved the highest total and excess volumetric H_2 storage with 50.69, 44.32 g/L at 77 K and 6.97, 2.49 g/L at 298 K. Besides, MIL-88B and D also achieved the high total H_2 storage at the value of 44.42 and 44.75 g/L at 77 K, respectively. The capacity for volumetric H_2 storage of MIL-88s, particularly MIL-88A, is worth noticing, and even very high in comparison to the other MOFs such as Be-MOF.

By substituting the metal component in MIL-88A with Sc, V, Ti, Cr, Mn and comparing with Fe and Co metals, calculations showed that Sc-MIL-88A achieved the highest absolute/excess uptakes that are 5.30/4.63 wt% at 77 K and 0.72/0.29 wt% at 298 K for gravimetric uptakes; 51.99/45.51 g/L at 77 K and 7.08/2.83 g/L at 298 K for volumetric uptakes. The hydrogen uptake is in the descending order that is Sc-, Ti-, V-, Cr-, Mn-, Fe-, and Co-MIL-88A, respectively.

Our results also exhibited that the gravimetric hydrogen uptakes depend on the special surface area and the pore volume of the MIL-88s, and apart depending on the type of the ligand.

6.2. Scientific contributions

This dissertation contributes to science by the following outcomes:

- We provide the approach combining DFT calculations and Murnaghan EOS to optimize the unit cell of MOFs.

- The overlapping between DOS curves of the adsorbed gas molecule and MOF is suggested to evaluate the interaction between them.

- The wave-function overlap between gas and the atoms of the MOF is used to show the gas – sorbent interaction.

- GCMC simulations show the gravimetric and volumetric uptakes of gas absorbed in MOFs as well as sorbents.

The calculation results show Sc-MIL-88A in the researched MIL-88 series is the best candidate for the volumetric hydrogen storage, while MIL-88D is the best one for gravimetric hydrogen storage.

6.3. Outlook

The initial results obtained for the hydrogen gas adsorption capacity in MIL-88 series are very promising. However, the amount of the adsorbed hydrogen gas in MIL-88s is still very low compared to the DOE targets, especially at room temperature; therefore, it should be improved to increase the amount of the adsorbed hydrogen gas. The following directions will be continued:

- Substitute Fe atoms in MIL-88D by other metals to improve H_2 adsorption capability.

- Replace the H atoms in the organic ligands of MIL-88s by functional groups such as -Cl, -F, -Br, -CH_2, *etc.* to increase the surface area of the MOF and enhance the hydrogen storage capacity.